European Review for Medical and Pharmacological Sciences 2020; 24: 97-108

MiR-140-5p and miR-92a-3p suppress the cell proliferation, migration and invasion and promoted apoptosis in Wilms' tumor by targeting FRS2

J.-L. LI[1], P. LUO[2]

[1]Department of Pediatrics, Cangzhou Central Hospital, Cangzhou, Hebei, China
[2]Department of CT, Cangzhou Central Hospital, Cangzhou, Hebei, China

Abstract. – OBJECTIVE: Wilms' tumor (WT) is the most common malignant renal tumor in children. MicroRNAs (MiRNAs) function in the progression of various cancers. Recent reports have reported that miR-140-5p and miR-92a-3p are dysregulated in WT tissues, but the potential mechanisms of the two miRNAs in modulating WT progression are still poorly understood.

MATERIALS AND METHODS: Quantitative Real Time-Polymerase Chain Reaction (qRT-PCR) was conducted to detect the expression levels of miR-140-5p, miR-92a-3p, and fibroblast growth factor receptor substrate 2 (FRS2) in WT tissues and cells, as well as matched controls. 3-(4, 5-dimethylthiazol-2-yl)-2, 5-diphenyltetrazolium bromide (MTT) assay and flow cytometry assay were employed to check cell proliferation and apoptosis, respectively. The abilities of cell migration and invasion were evaluated by transwell assay. The protein level of FRS2 in samples was measured by Western blot. The starBase was used to predict the binding sites between FRS2 and miR-140-5p or miR-92a-3p and the Dual-Luciferase reporter assay was performed to verify the interaction. Xenograft tumor model was established to investigate the biological roles of the two miRNAs in WT *in vivo*.

RESULTS: The levels of miR-140-5p and miR-92a-3p were significantly downregulated in WT tissues and cells, while the expression of FRS2 was significantly upregulated. The two miRNAs both inhibited proliferation, migration, invasion, and induced apoptosis of WT cells. Besides, FRS2 was a target of the two miRNAs and its overexpression reversed the effects of the two miRNAs-mediated suppression on WT progression. Moreover, the upregulation of the two miRNAs repressed tumor growth *in vivo*.

CONCLUSIONS: MiR-140-5p and miR-92a-3p attenuated the aggressive progression of WT *via* targeting FRS2.

Key Words:
WT, MiR-140-5p, MiR-92a-3p, FRS2.

Introduction

Wilms' tumor (WT), also called nephroblastoma, mainly occurs in children and its peak age is 3 to 4 years. However, most cases occurr before the age of 10 years[1,2]. Although the overall five-year survival rate is high[3], some children die due to recurrence, and the relapse rate is close to 15%[4]. Hence, it is still essential to find novel therapeutic methods and molecular targets for WT treatment.

MicroRNAs (MiRNAs) are short (about 22 nucleotides) and highly conserved noncoding RNAs, which modulate gene expression by guiding Argonaute proteins to target sites in the 3'-untranslated region (3'UTR) of messenger RNA (mRNA)[5]. MiRNAs are involved in diverse human cancers[6,7] and can act as oncogenes or tumor suppressors according to their target genes[8]. MiR-140-5p was reported to be associated with gastric cancer[9] and hepatocellular carcinoma[10]. MiR-92a-3p participated in the progression of liposarcoma[11] and colorectal cancer[12]. Recent research[13-15] showed that both miR-140-5p and miR-92a-3p were downregulated in WT tissues. However, the underlying regulatory mechanisms of the two miRNAs in WT progression have not been fully uncovered.

Fibroblast growth factor receptor substrate 2 (FRS2), belonging to adaptors/scaffold protein family, is correlated with the disappointing outcome of numerous human cancers. Wu et al[16] found that FRS2 duplication was an adverse prognostic factor for the survival of bladder cancer patients. Luo et al[17] showed that FRS2 played an oncogenic role in ovarian cancer. Also, Wang et al[18] reported that FRS2 was overexpressed in

Corresponding Author: Jinling Li, MM; e-mail: bewvgy@163.com

WT tissues. Therefore, FRS2 may be an appealing WT drug target and it deserves to be further studied.

In this research, the levels of miR-140-5p, miR-92a-3p, and FRS2 in WT tissues and cells were measured. The functions and potential regulatory mechanisms of the two miRNAs in WT were investigated by bioinformatics analysis and subsequent experiments.

Material and Methods

Samples and Cell Culture

WT tissues and nearby non-cancerous tissues were collected from Cangzhou Central Hospital. The informed consent was acquired from every patient and this research was approved by the Ethics Committee of the Cangzhou Central Hospital. Human normal renal tubular epithelial cell line (HK-2) was purchased from China Center for Type Culture Collection (Wuhan, China); human WT cell lines (WiT49 and 17-94) were obtained from Thermo Fisher Scientific (Waltham, MA, USA) and DSMZ (Lower Saxony, Braunschweig, Germany), respectively. McCoy's 5A medium (Sigma-Aldrich, St. Louis, MO, USA), containing 5% CO_2 and 10% fetal bovine serum (FBS) (Sigma-Aldrich, St. Louis, MO, USA) was utilized to culture cells.

Cell Transfection

MiR-140-5p mimic (named as miR-140-5p), miR-92a-3p mimic (named as miR-92a-3p), and small interfering RNA against FRS2 (named as si-FRS2), as well as their corresponding controls, were obtained from GenePharma (Shanghai, China). FRS2 expression plasmid (named as FRS2) and its matched control (named as pcDNA) were acquired from RiboBio (Guangzhou, China). Cell transfection was performed using Lipofectamine 2000 reagent (Invitrogen, Carlsbad, CA, USA) following the given procedures.

RNA Isolation and Quantitative Real Time-Polymerase Chain Reaction (qRT-PCR)

WT tissues and cells were collected, and the total RNA was extracted using the TRIzol reagent (Vazyme, Nanjing, China). Then, RNA was reversely transcribed to complementary DNA (cDNA) by PrimeScript™ RT Master Mix kit (TaKaRa, Dalian, China). The qRT-PCR was conducted by SYBR Green PCR Master Mix (Vazyme, Nanjing, China) and data were analyzed using $2^{-\Delta\Delta Ct}$ method. Beta-actin (β-actin) and U6 were introduced as the inner references. The primers used in this study:

miR-140-5p (forward 5'-TGCGGCAGTG-GTTTTACCCTATG-3', reverse 5'-CCAGTGCAG-GGTCCGAGGT-3'); miR-92a-3p (forward, 5'-GGG-GCAGTTATTGCACTTGTC-3', reverse 5'-CCAGT-GCAGGGTCCGAGGTA-3'); FRS2 (forward, 5'-GTGCCGCATCTTTACCCTCA-3', reverse5'-TC-GCCATTAAATTCTGGCTGC-3'); β-actin (forward 5'-GCACCACACCTTCTACAATG-3',reverse, 5'-TGCTTGCTGATCCACATCTG-3'); U6 (forward, 5'-TCCGGGTGATGCTTTTCCTAG-3', reverse, 5'-CGCTTCACGAATTTGCGTGTCAT-3').

3-(4,5-Dimethylthiazol-2-yl)-2,5-Diphenyltetrazolium Bromide (MTT) Assay

In brief, the transfected cells were sowed into 96-well plates and were incubated for the different time. Next, 20 μL MTT solution (5 mg/mL) (Sigma-Aldrich, St. Louis, MO, USA) was added to each well to incubate for 4 h, and then, each well was filled with 200 μL dimethyl sulfoxide (DMSO; Sigma-Aldrich, St. Louis, MO, USA) after discarding medium. Optical density values were examined at 490 nm wavelength under the microplate reader (Bio-Rad, Hercules, CA, USA).

Flow Cytometry

Annexin Apoptosis Detection Kit (Sigma-Aldrich, St. Louis, MO, USA) was utilized to check cell apoptosis following the given procedures. Briefly, the cells were resuspended using the binding buffer, and then, 5 μL Annexin V-fluorescein isothiocyanate (Annexin V-FITC) and 5 μL propidium iodide (PI) were added to the buffer and incubated for 5 min in the dark. The stained cells were analyzed by flow cytometry (Countstar®, Shanghai, China).

Transwell Assay

Transwell chamber precoated with Matrigel (Corning Life Sciences, Corning, NY, USA) or not was employed to check the capacity of cell invasion or migration, respectively. Transfected cells were seeded into the upper chamber and the medium containing fetal bovine serum (FBS) was placed in the lower chamber. After being treated with crystal violet (Solarbio, Beijing, China), migrated or invaded cells were analyzed under an inverted microscope (MTX Lab Systems, Bradenton, FL, USA).

Western Blot

Proteins from samples were isolated using RIPA buffer (Vazyme, Nanjing, China) and the protein concentration was checked by Detergent Compatible Bradford Protein Quantification Kit (Vazyme, Nanjing, China). The proteins were segregated by sodium dodecyl sulfate polyacrylamide gel electrophoresis (SDS-PAGE), and then, transferred onto the polyvinylidene difluoride (PVDF) membranes (Vazyme, Nanjing, China). The membranes were blocked with 5% skimmed milk (Vazyme, Nanjing, China) and washed by phosphate-buffered saline (PBS). Afterwards, the membranes were incubated with the primary antibodies: anti-FRS2 (1:2000, ab137458, Abcam, Cambridge, UK) or glyceraldehyde 3-phosphate dehydrogenase (GAPDH) (1:2500, ab9485, Abcam, Cambridge, UK) overnight. After being rewashed, the membranes were incubated with the secondary antibody (1:3000, ab205718, Abcam, Cambridge, UK) for 3 h. The membranes were analyzed by the ChemiDoc™ MP Imaging System (Bio-Rad, Hercules, CA, USA) after being treated with ECL kit (Vazyme, Nanjing, China).

Dual-Luciferase Reporter Assay

The potential complementary sequences between FRS2 and miR-140-5p or miR-92a-3p were forecasted by starBase[19]. The wild type sequence of FRS2 3'UTR harboring the binding sites of the two miRNAs was inserted into the pGL3 vector (Promega, Madison, WI, USA) to construct the Luciferase reporter vector FRS2 3'UTR-WT. Similarly, FRS2 3'UTR-MUT reporter vector was established by mutating the potential target sites of the two miRNAs. Then, the vectors with miR-140-5p or miR-92a-3p, as well as corresponding controls, were cotransfected into WiT49 and 17-94 cells using Lipofectamine 2000 (Invitrogen, Carlsbad, CA, USA). The Dual-Glo® Luciferase Assay System kit (Promega, Madison, WI, USA) was utilized to measure Luciferase activity.

Xenograft Mice Models

Six-week-old BALB/c nude mice were acquired from Vital River Laboratory Animal Technology (Beijing, China). WiT49 cells stably infected with miR-140-5p, miR-92a-3p or miR-NC were injected subcutaneously into the flank of the nude mice. The tumor volume was calculated every 4 d according to the formula: $0.5 \times \text{length} \times \text{width}^2$. The tumor weight was measured after the mice were euthanized and the mRNA and protein levels of FRS2 in tumors were checked by qRT-PCR. The animal experiment was approved by the Animal Care and Use Committee of Cangzhou Central Hospital and performed following the instructions of the National Animal Protection and Ethics Institute.

Statistical Analysis

Experimental data were calculated by GraphPad Prism (GraphPad, La Jolla, CA, USA) and presented by mean ± standard deviation (SD). Two independent groups were compared by using Student's *t*-test. For more than two groups, the One-way analysis of variance (ANOVA) followed by Tukey's test was utilized to assess the difference. Every experiment was repeated at least three times independently. $p < 0.05$ represented statistical significance.

Results

MiR-140-5p and MiR-92a-3p Were Strikingly Downregulated in WT Tissues and Cells

To investigate the roles of miR-140-5p and miR-92a-3p, we measured their expression levels in WT tissues and cells. The data showed that miR-140-5p was conspicuously downregulated in WT tissues and cells compared with corresponding normal tissues and cells (Figure 1A and 1B). Similarly, the expression level of miR-92a-3p was also significantly elevated in WT tissues and cells compared with matched controls (Figure 1C and 1D). Together, these results supported the idea that miR-140-5p and miR-92a-3p might serve as tumor suppressors in the progression of WT.

MiR-140-5p and MiR-92a-3p Inhibited Proliferation, Migration, Invasion and Boosted Apoptosis of WT Cells

To study the possible roles of miR-140-5p and miR-92a-3p in WT cell proliferation, apoptosis, migration, and invasion, WT cells were transfected with miR-140-5p, miR-92a-3p or miR-NC, and the knockdown efficiency was tested by qRT-PCR (Figure 2A and 2B). MTT assay showed that the proliferation of WiT49 and 17-94 cells was apparently suppressed in miR-140-5p and miR-92a-3p groups compared with the miR-NC group (Figure 2C and 2D). Flow cytometry assay revealed that the apoptosis rates of WT cells transfected with miR-140-5p or miR-92a-3p were notably increased (Figure 2E). In addition, transwell assay illustrated that the upregulation

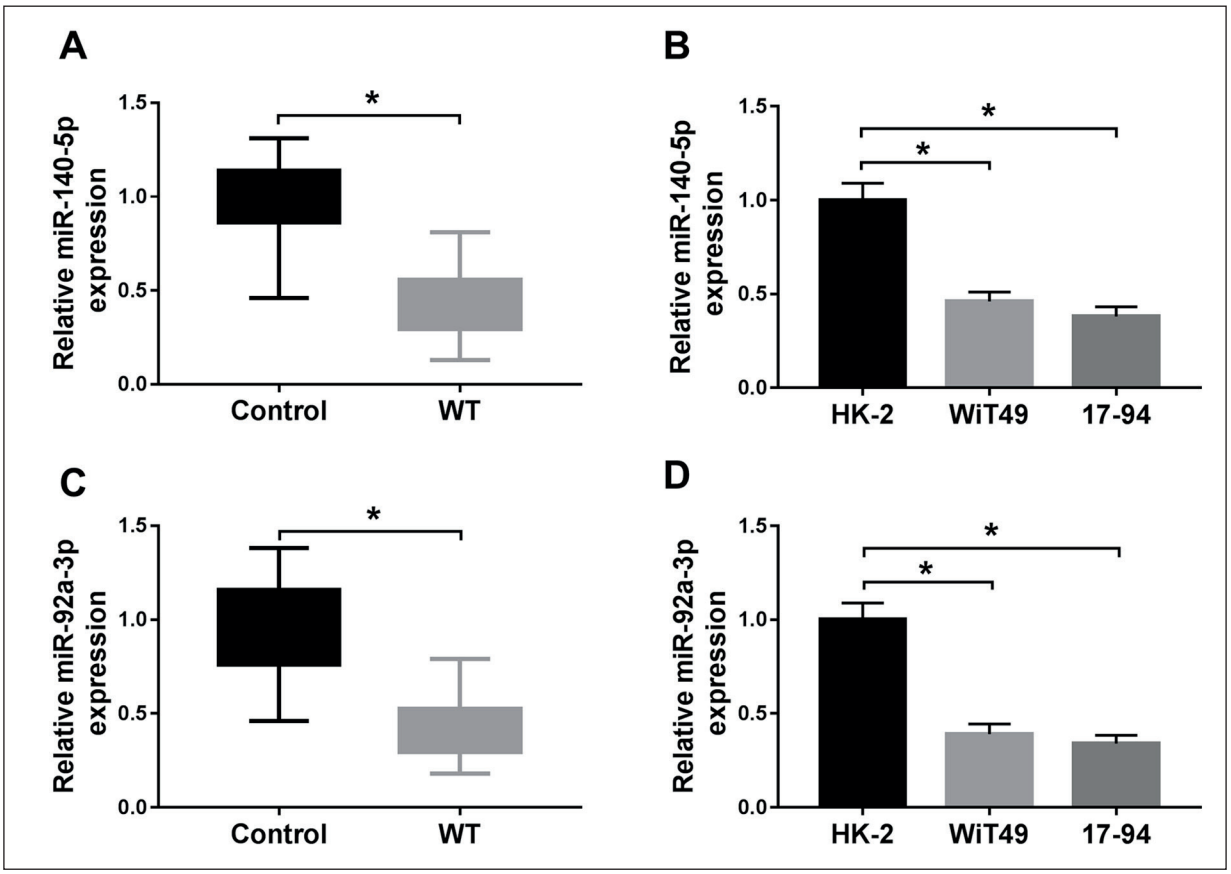

Figure 1. MiR-140-5p and miR-92a-3p were downregulated in WT tissues and cells. **A,** and **B,** The expression of miR-140-5p in WT tissues and cells was detected by qRT-PCR. **C,** and **D,** The level of miR-92a-3p in WT tissues and cells was checked by qRT-PCR. *$p<0.05$.

of miR-140-5p or miR-92a-3p inhibited migration and invasion of WT cells (Figure 2F and 2G). Collectively, these results demonstrated that miR-140-5p and miR-92a-3p exerted inhibitory effects on the progression of WT *in vitro*.

FRS2 Was Upregulated in WT Tissues and Cells and Its Knockdown Suppressed WT Progression

To study the possible function of FRS2 in WT progression, the mRNA and protein levels of FRS2 in WT tissues and cells were assessed by qRT-PCR and Western blot, respectively. The results showed that the mRNA and protein levels of FRS2 were both markedly elevated in WT tissues and cells compared with normal tissues and cells (Figure 3A-3D). Subsequently, the expression of FRS2 in WT cells transfected with si-FRS2 or si-NC was checked, and the results indicated that the mRNA and protein levels of FRS2 were both dramatically declined in si-FRS2 group (Figure 3E and 3F). MTT assay manifested that reducing the expression of FRS2 repressed proliferation of WiT49 and 17-94 cells (Figure 3G and 3H). Moreover, the apoptosis rates of WT cells were strikingly elevated in the si-FRS2 group (Figure 3I). Further analysis elucidated that the knockdown of FRS2 weakened the capacities of migration and invasion of WT cells (Figure 3J and 3K). These results suggested that FRS2 silencing repressed proliferation, migration, invasion and promoted apoptosis of WT cells.

FRS2 Was a Target of MiR-140-5p and MiR-92a-3p, and Was Negatively Modulated by the Two MiRNAs

To deeply explore the regulatory mechanisms of the two miRNAs in WT progression, starBase was utilized to find their potential target genes. The result showed that miR-140-5p could bind to the 3'UTR of FRS2 (Figure 4A). Then, the Dual-Luciferase reporter assay was introduced to confirm the prediction and the data indicated that miR-140-5p significantly diminished the Lu-

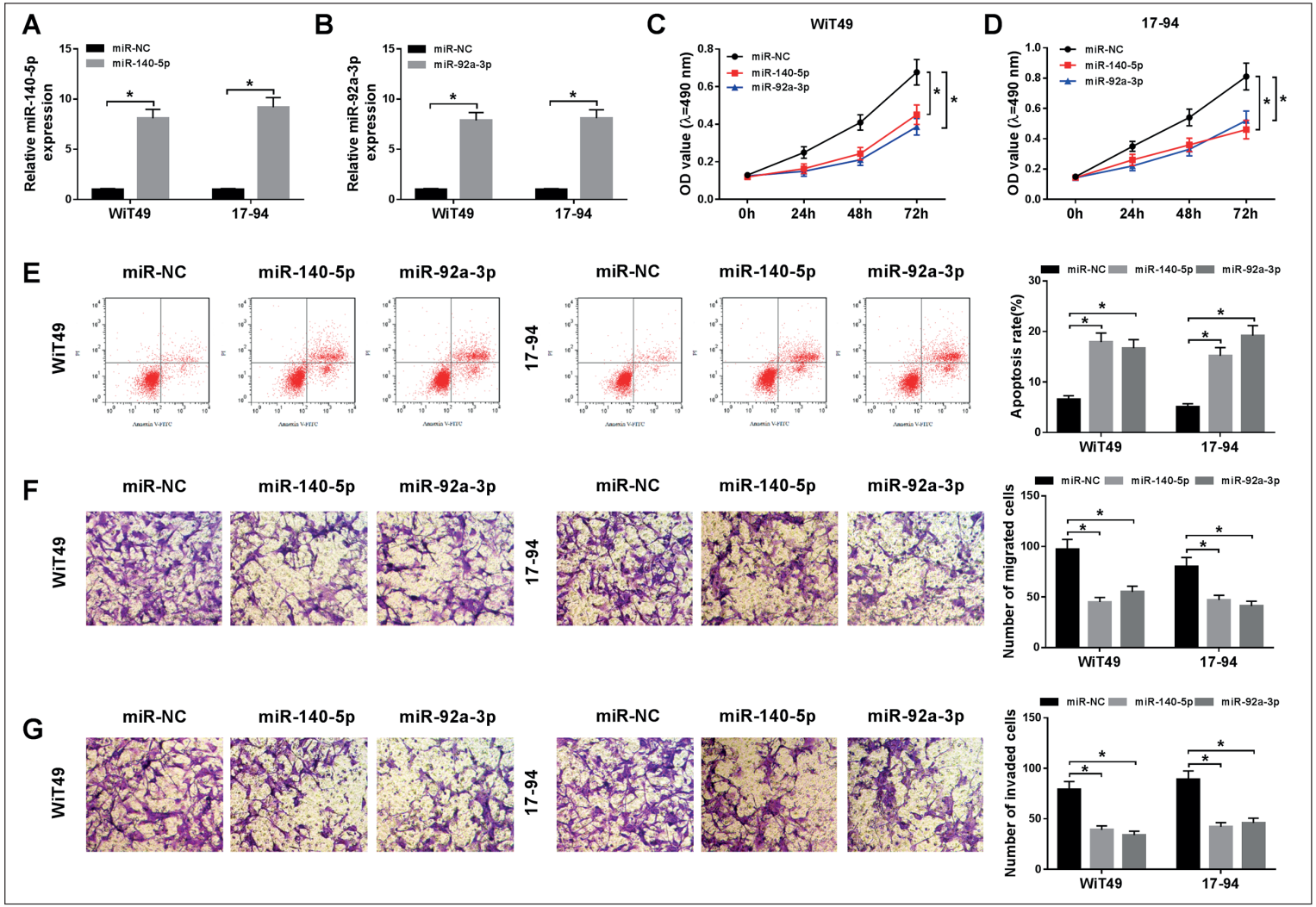

Figure 2. MiR-140-5p and miR-92a-3p hampered WT progression. **A,** and **B,** The expression of miR-140-5p and miR-92a-3p in WT cells infected with miR-140-5p, miR-92a-3p or miR-NC was measured by qRT-PCR. **C,** and **D,** The proliferation of infected WT cells was assessed by MTT assay. **E,** The apoptosis of infected WT cells was checked by flow cytometry. **F,** and **G,** Transwell assay was employed to measure the abilities of cell migration and invasion (100×). *$p<0.05$.

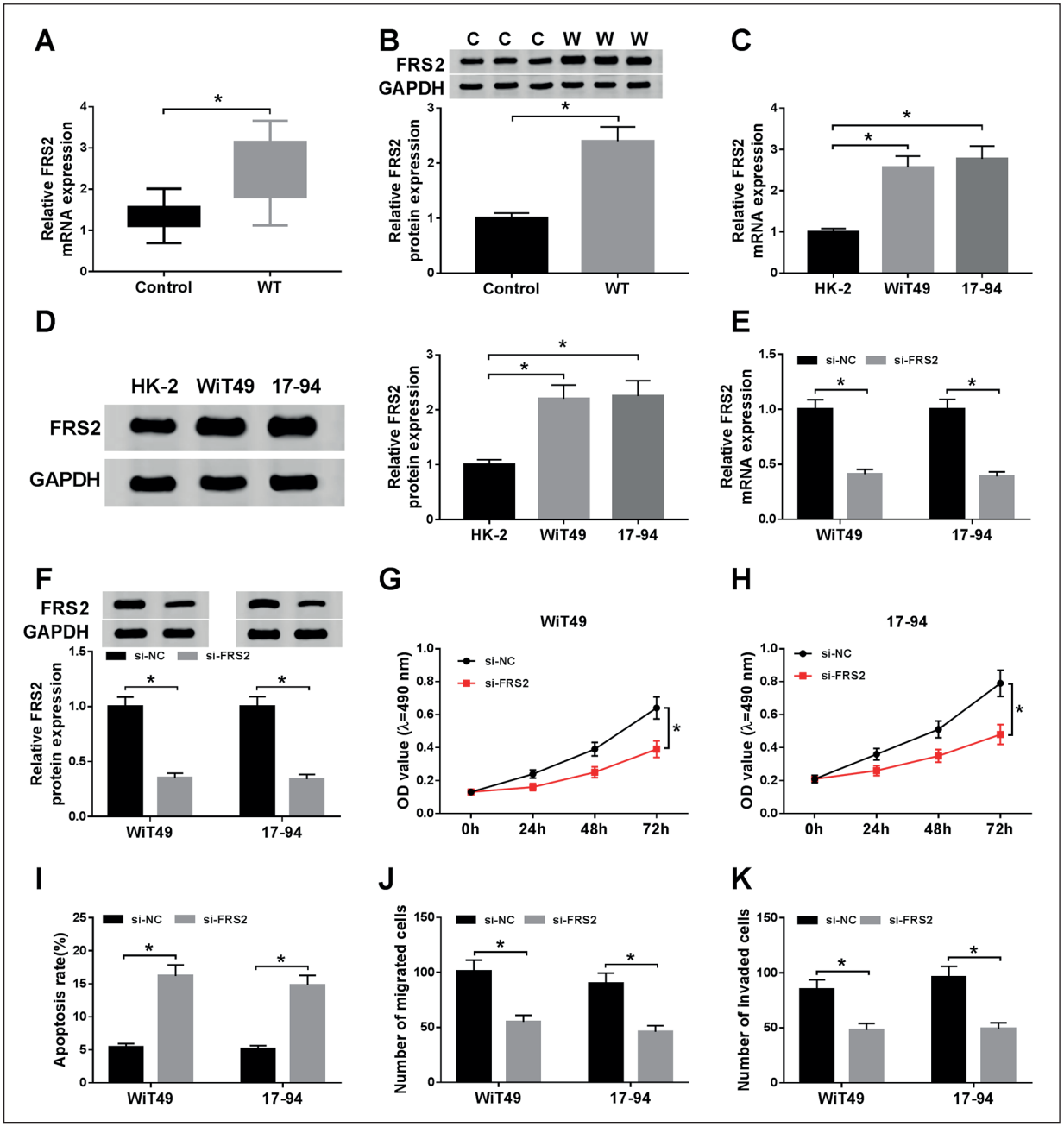

Figure 3. FRS2 silencing inhibited WT progression. **A,** and **B,** The mRNA and protein levels of FRS2 in WT tissues were measured by qRT-PCR and Western blot, respectively. **C,** and **D,** The mRNA and protein levels of FRS2 in WT cells were determined by qRT-PCR and Western blot, respectively. **E,** and **F,** The mRNA and protein levels of FRS2 in WT cells transfected with si-FRS2 or si-NC were checked by qRT-PCR and Western blot, respectively. **G,** and **H,** MTT assay was employed to evaluate cell proliferation. **I,** Flow cytometry was hired to analyze cell apoptosis. **J,** and **K,** Transwell assay was employed to measure the abilities of cell migration and invasion, and the corresponding cell numbers were calculated. *p<0.05.

ciferase activity of FRS2 3'UTR-WT in WiT49 and 17-94 cells, rather than FRS2 3'UTR-MUT (Figure 4B and 4C). Besides, the expression of miR-140-5p was negatively associated with FRS2 in WT tissues (Figure 4D), and the mRNA and protein levels of FRS2 were both downregulated in WT cells infected with miR-140-5p (Figure 4E and 4F). Interestingly, FRS2 was also predicted to be a target of miR-92a-3p (Figure 4G), and the interaction was verified by the Dual-Luciferase reporter assay (Figure 4H and 4I). Similarly, miR-92a-3p was negatively correlated with FRS2

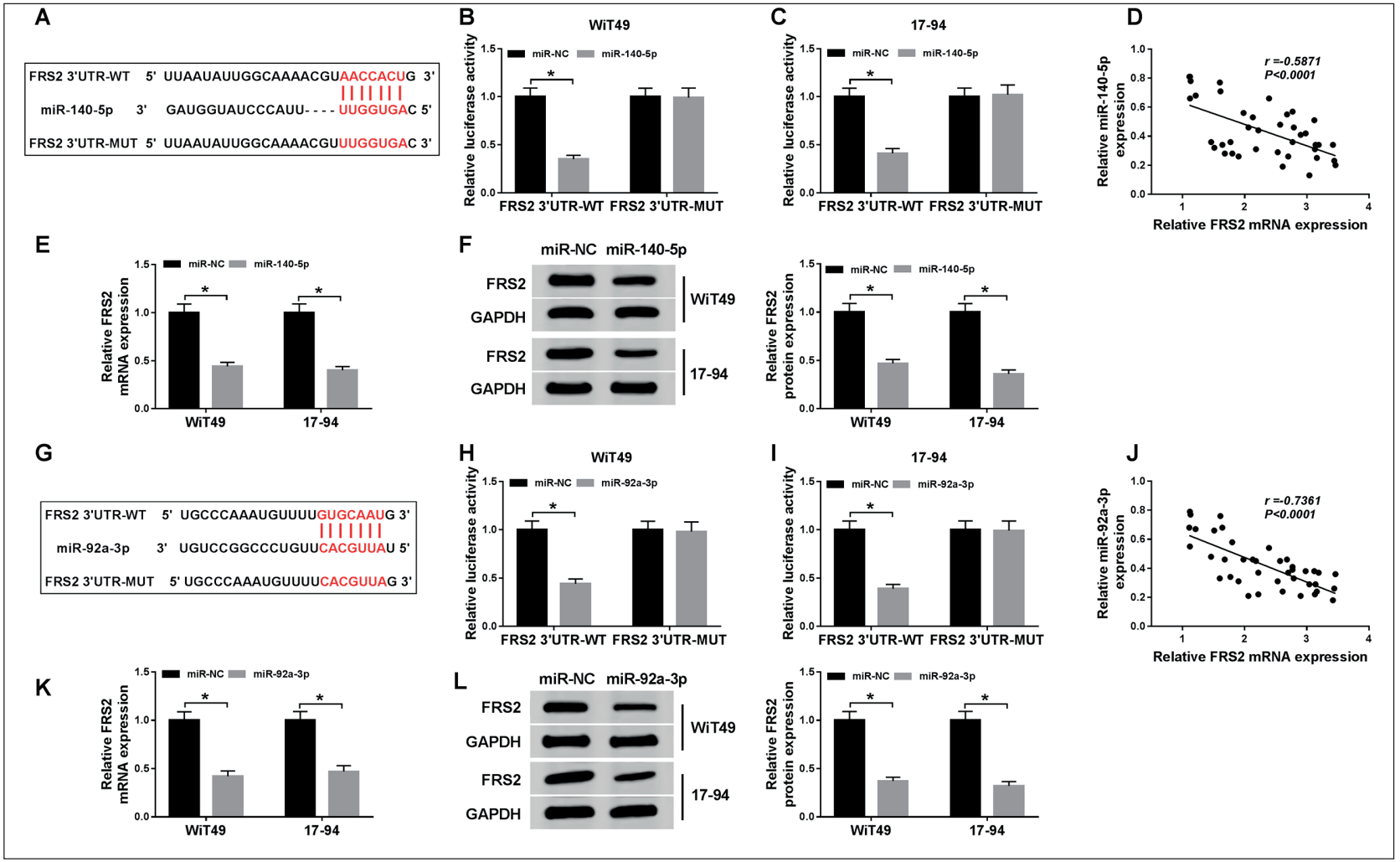

Figure 4. MiR-140-5p and miR-92a-3p targeted the 3'UTR of FRS2 in WT cells *in vitro*. **A,** The interaction between miR-140-5p and FRS2 was forecasted by starBase. **B,** and **C,** The Dual-Luciferase reporter assay was used to check the Luciferase activity of WT cells cotransfected with miR-140-5p or miR-NC and FRS2 3'UTR-WT or FRS2 3'UTR-MUT. **D,** The correlation between miR-140-5p and FRS2 in WT tissues was analyzed using Pearson's correlation coefficient. **E,** and **F,** The mRNA and protein levels of FRS2 in WT cells transfected with miR-140-5p or miR-NC were measured by qRT-PCR and Western blot, respectively. **G,** The interaction between miR-92a-3p and FRS2 was predicted by starBase. **H,** and **I,** The dual-luciferase reporter assay was performed to confirm the interaction between miR-92a-3p and FRS2. **J,** The correlation between miR-92a-3p and FRS2 in WT tissues was analyzed using Pearson's correlation coefficient. **K,** and **L,** The mRNA and protein levels of FRS2 in WT cells transfected with miR-92a-3p or miR-NC were checked by qRT-PCR and Western blot, respectively. *$p<0.05$.

in WT tissues (Figure 4J), and upregulation of miR-92a-3p decreased the mRNA and protein levels of FRS2 in WT cells (Figure 4K and 4L). To sum up, these results disclosed that both miR-140-5p and miR-92a-3p could target the 3'UTR of FRS2 and negatively regulated the expression of FRS2 *in vitro*.

Overexpression of FRS2 Reversed the Effects of MiR-140-5p- and MiR-92a-3p-Mediated Inhibition on WT Progression

To figure out the role of the interaction between the two miRNAs and FRS2 in WT progression, we first checked the mRNA and protein expression levels of FRS2 in WT cells infected with miR-140-5p or miR-140-5p + FRS2, as well as matched controls. The data showed that FRS2 was evidently downregulated in the miR-140-5p group, while its expression level was clearly overturned after the transfection with FRS2 (Figure 5A-5B). In addition, upregulation of FRS2 reversed the impact of miR-140-5p-mediated inhibition on proliferation of WT cells (Figure 5C and 5D). Apoptosis assay elucidated that FRS2 overexpression abolished the promoted effect of miR-140-5p on apoptosis of WT cells (Figure 5E). Besides, enforced expression of FRS2 revoked the effects of miR-140-5p-mediated repression on migration and invasion of WT cells (Figure 5F and 5G). Simultaneously, similar phenomena were observed from miR-92a-3p. The expression of FRS2 in miR-92a-3p group was inverted after the transfection with FRS2 (Figure 5H and 5I). Overexpression of FRS2 rescued miR-92a-3p-mediated and repressed effect on proliferation of WT cells (Figure 5J and 5K), and transposed miR-92a-3p-induced apoptosis of WT cells (Figure 5L). Moreover, the effects of miR-92a-3p-mediated suppression on migration and invasion were overset by upregulating FRS2 (Figure 5M and 5N). Taken together, these results elucidated that FRS2 and the two miRNAs played opposite roles in WT, and overexpression of FRS2 impaired miR-140-5p- and miR-92a-3p-mediated inhibitory effects on the progression of WT.

Upregulation of MiR-140-5p and MiR-92a-3p Retarded Tumor Growth In Vivo

To confirm the functions of miR-140-5p and miR-92a-3p in WT progression *in vivo*, we established the xenograft mouse models using WT cells transfected with miR-140-5p, miR-92a-3p, or miR-NC. The data showed that miR-140-5p mimic led to clear shrink in tumor volume (Figure 6A) and decline in tumor weight (Figure 6B). Then, the expression levels of miR-140-5p and FRS2 in tumors were measured, and the results indicated that the expression of miR-140-5p was apparently increased in miR-140-5p group compared with miR-NC group (Figure 6C), which was contrary to the expression of FRS2 (Figure 6D and 6E). Similarly, the upregulation of miR-92a-3p reduced the volume and weight of tumors (Figure 6F and 6G) and miR-92a-3p was upregulated in WT cells transfected with miR-92a-3p (Figure 6H). The mRNA and protein levels of FRS2 were clearly declined in miR-92a-3p group (Figure 6I and 6J). In summary, miR-140-5p and miR-92a-3p could hinder tumor growth *in vivo*.

Discussion

WT generally occurs in early childhood and has a peak incidence at 3 to 4 years old[20]. Even though the survival rate is elevated, a few children die of recurrence and the relapse rate is up to 15%[4]. Therefore, it is still essential to find more molecular targets and dissect underlying mechanisms, which may contribute to the development of more effective and safer drugs for WT.

MiRNAs have been confirmed to participate in the progression of various cancers[6,7] and are usually abnormal expressed[21,22]. MiR-140-5p and miR-92a-3p played pivotal roles in cancer progression. Fang et al[9] reported that miR-140-5p suppressed viability and metastasis of gastric cancer cells. Yang et al[10] confirmed that miR-140-5p obstructed the growth of hepatocellular carcinoma. Casadei et al[11] reported that exosome-derived miR-92a-3p stimulated liposarcoma progression. Another study indicated that miR-92a-3p was an early biomarker for detecting hepatocellular carcinoma[23]. To study the functions of the two miRNAs, we first checked their expression in WT tissues and cells, as well as corresponding controls. The results showed that the two miRNAs were both apparently downregulated in WT tissues and cells, which was in line with previous reports[13-15]. Further studies suggested that miR-140-5p and miR-92a-3p suppressed proliferation, migration, invasion, and accelerated apoptosis of WT cells. In addition, the two miRNAs handicapped tumor growth *in vivo*. These results illustrated that miR-140-5p and miR-92a-3p functioned as tumor suppressors in WT progression.

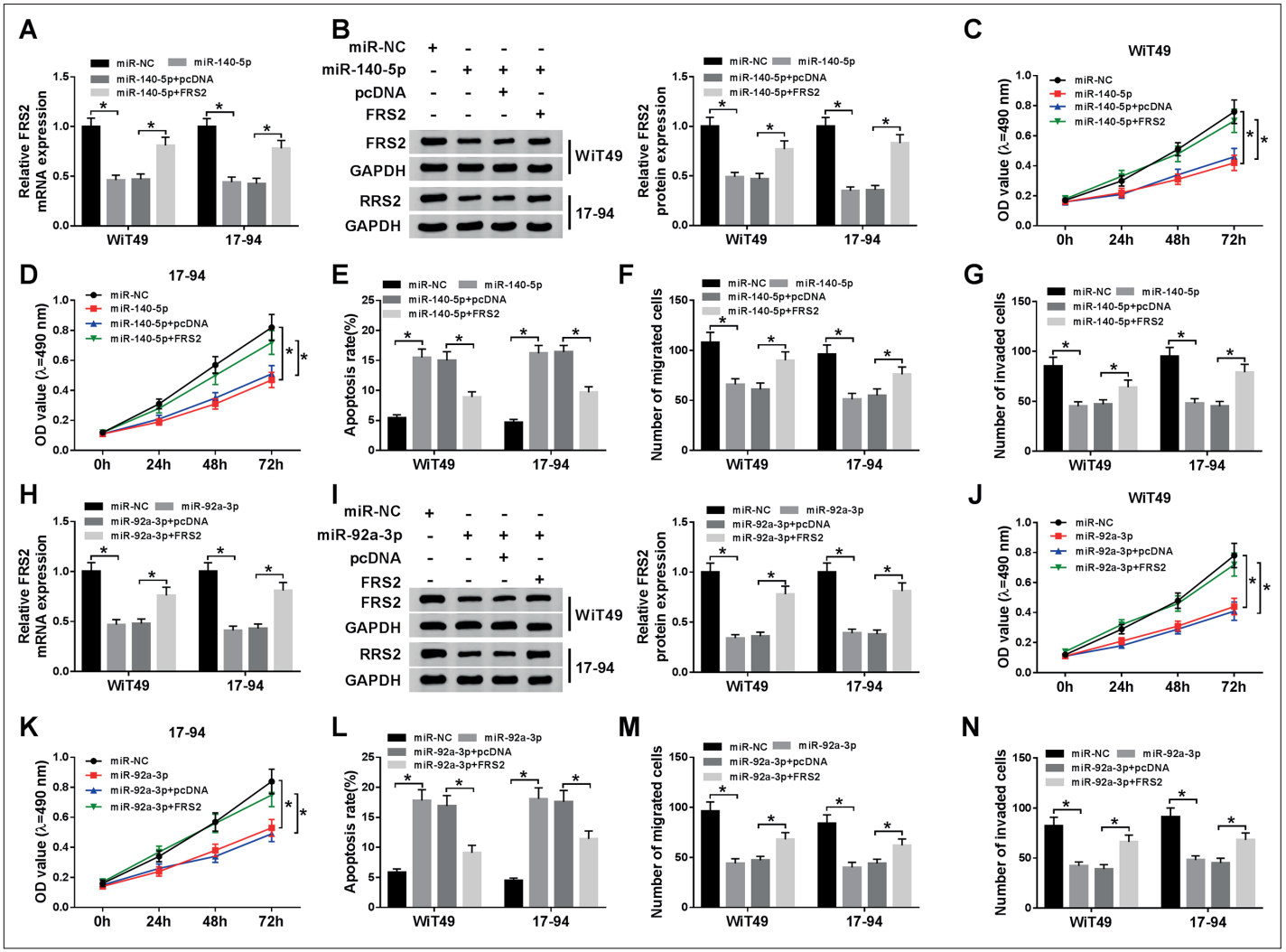

Figure 5. Overexpression of FRS2 inverted the inhibitory effects of miR-140-5p and miR-92a-3p on WT progression. **A,** and **B,** The mRNA and protein levels of FRS2 in WT cells transfected with miR-140-5p or miR-140-5p + FRS2, as well as matched controls, were measured by qRT-PCR and Western blot, respectively. **C,** and **D,** Proliferation of transfected WT cells was evaluated by MTT assay. **E,** Apoptosis of transfected WT cells was analyzed by flow cytometry. **F,** and **G,** Transwell assay was utilized to measure the abilities of cell migration and invasion. **H,** and **I,** The mRNA and protein levels of FRS2 in WT cells transfected with miR-92a-3p or miR-92a-3p + FRS2, as well as corresponding controls, were checked by qRT-PCR and Western blot, respectively. **J,** and **K,** Cells proliferation was evaluated by MTT assay. **L,** Flow cytometry was conducted to check apoptosis of transfected WT cells. **M,** and **N,** Transwell assay was carried out to assess the abilities of cell migration and invasion. *$p<0.05$.

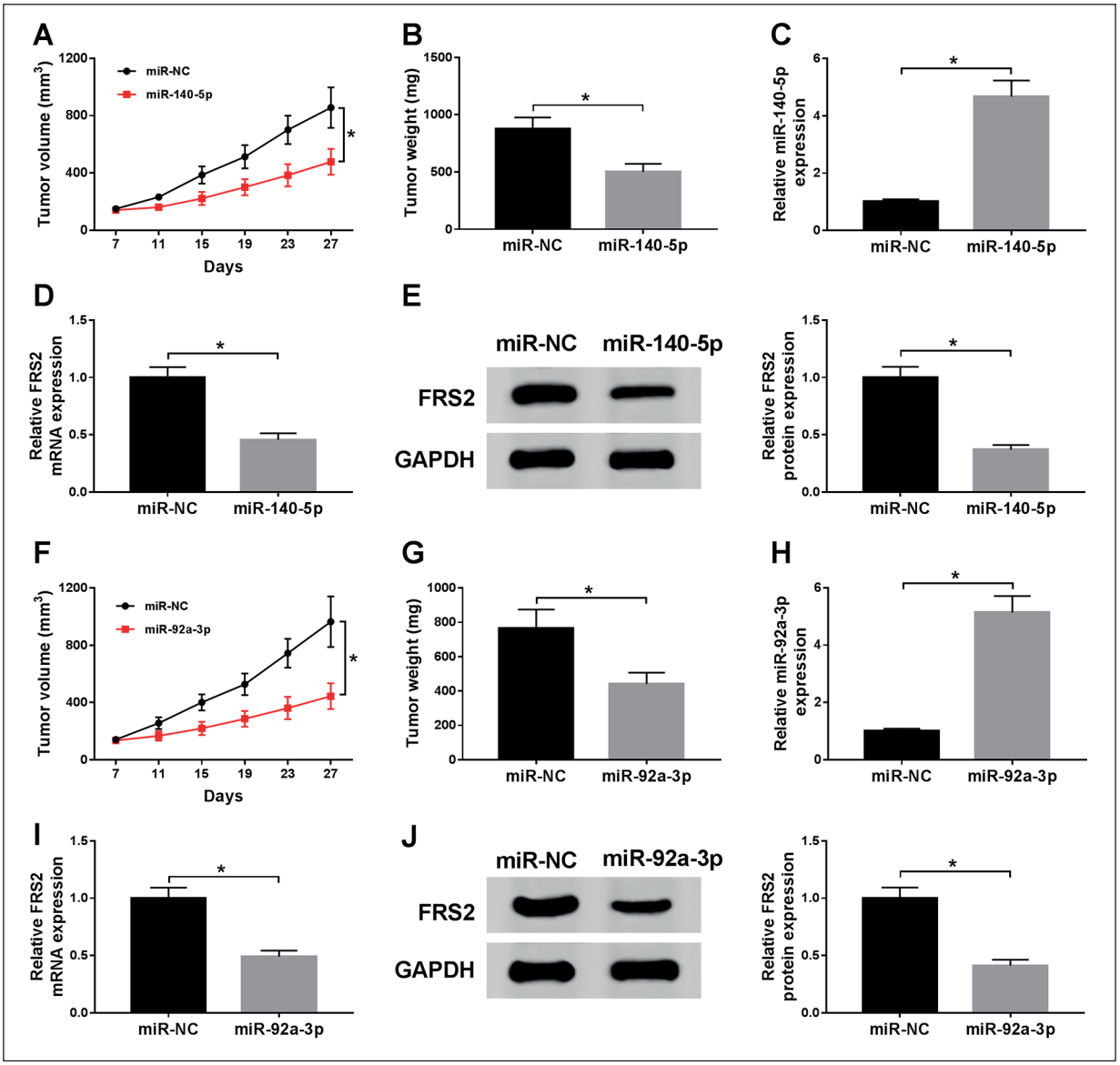

Figure 6. Mir-140-5p and miR-92a-3p blocked tumor growth *in vivo*. **A,** Tumor volume was measured every 4 d after subcutaneous injection with miR-140-5p or miR-NC. **B,** Weight of the resected tumor was examined after the mice were killed. **C,** The level of miR-140-5p in WT cells transfected with miR-140-5p or miR-NC was measured by qRT-PCR. **D,** and **E,** The mRNA and protein levels of FRS2 in transfected WT cells were determined by qRT-PCR and Western blot, respectively. **F,** Tumor volume was measured every 4 d after subcutaneous injection with miR-92a-3p or miR-NC. **G,** Weight of the resected tumor was measured after the mice were killed. **H,** The expression of miR-92a-3p in WT cells transfected with miR-92a-3p or miR-NC was checked by qRT-PCR. **I,** and **J,** The mRNA and protein levels of FRS2 in transfected WT cells were measured by qRT-PCR and Western blot, respectively. *$p<0.05$.

FRS2 is an adaptor protein and functions in epidermal growth factor signaling[24]. Recent studies indicated that FRS2 was closely related to human cancers. Wu et al[16] disclosed that FRS2 duplication led to poor prognosis of bladder cancer. Zhang et al[25] reported that FRS2 was amplified in high-grade liposarcoma cells. Luo et al[17] confirmed that FRS2 was upregulated and served as an oncogene in advanced ovarian cancers. In this research, the expression of FRS2 was notably increased in WT tissues and cells, which was supported by Wang et al[18]. Moreover, the knockdown of FRS2 hampered proliferation, migration, invasion, and boosted apoptosis of WT cells. From these results, it could be concluded that FRS2 acted as an oncogene in WT progression.

Bioinformatic analysis showed that FRS2 was a target of miR-140-5p and miR-92a-3p, and the interaction was corroborated by the Dual-Luciferase reporter assay. Correlation analysis indicated that the expression of FRS2 was negatively correlated with the two miRNAs in WT tissues. Intensive studies illustrated that miR-140-5p and miR-92a-3p markedly decreased the expression of FRS2 in WT cells, while the overexpression of FRS2 inverted this effect. Also, the upregulation of FRS2 reversed the impacts of the two miRNAs-mediated suppression on proliferation, migration, invasion, and promotion on apoptosis of WT cells. Moreover, enhancement of miR-140-5p and miR-92a-3p downregulated the expression of FRS2 and repressed cancer growth *in vivo*. Taken together, these results suggested that miR-140-5p and miR-92a-3p could interact with and downregulate FRS2, which played an oncogenic role, thus damaging the progression of WT.

Conclusions

Our research showed that miR-140-5p and miR-92a-3p were significantly decreased in WT tissues and cells, and the two miRNAs could inhibit WT progression by targeting the 3'UTR of FRS2. This novel regulatory mechanism may provide effective therapeutic methods for WT.

Conflict of Interest

The Authors declare that they have no conflict of interests.

References

1) Breslow NE, Beckwith JB, Perlman EJ, Reeve AE. Age distributions, birth weights, nephrogenic rests, and heterogeneity in the pathogenesis of Wilms tumor. Pediatr Blood Cancer 2006; 47: 260-267.
2) Sonn G, Shortliffe LMD. Management of Wilms tumor: current standard of care. Nat Clin Pract Urol 2008; 5: 551.
3) Stewénius Y, Jin Y, Øra I, de Kraker J, Bras J, Frigyesi A, Alumets J, Sandstedt B, Meeker AK, Gisselsson D. Defective chromosome segregation and telomere dysfunction in aggressive Wilms' tumors. Clin Cancer Res 2007; 13: 6593-6602.
4) Maschietto M, Piccoli FS, Costa CM, Camargo LP, Neves JI, Grundy PE, Brentani H, Soares FA, Camargo B, Carraro DM. Gene expression analysis of blastemal component reveals genes associated with relapse mechanism in Wilms tumour. Eur J Cancer 2011; 47: 2715-2722.
5) Gebert LFR, MacRae IJ. Regulation of microRNA function in animals. Nat Rev Mol Cell Biol 2019; 20: 21-37.
6) Grigelioniene G, Suzuki HI, Taylan F, Mirzamohammadi F, Borochowitz ZU, Ayturk UM, Tzur S, Horemuzova E, Lindstrand A, Weis MA, Grigelionis G, Hammarsjö A, Marsk E, Nordgren A, Nordenskjöld M, Eyre DR, Warman ML, Nishimura G, Sharp PA, Kobayashi T. Gain-of-function mutation of microRNA-140 in human skeletal dysplasia. Nat Med 2019; 25: 583-590.
7) Iorio MV, Visone R, Di Leva G, Donati V, Petrocca F, Casalini P, Taccioli C, Volinia S, Liu CG, Alder H, Calin GA, Ménard S, Croce CM. MicroRNA signatures in human ovarian cancer. Cancer Res 2007; 67: 8699-8707.
8) Peng Y, Croce CM. The role of MicroRNAs in human cancer. Signal Transduct Target Ther 2016; 1: 15004.
9) Fang Z, Yin S, Sun R, Zhang S, Fu M, Wu Y, Zhang T, Khaliq J, Li Y. MiR-140-5p suppresses the proliferation, migration and invasion of gastric cancer by regulating YES1. Mol Cancer 2017; 16: 139.
10) Yang H, Fang F, Chang R, Yang L. MicroRNA-140-5p suppresses tumor growth and metastasis by targeting transforming growth factor β receptor 1 and fibroblast growth factor 9 in hepatocellular carcinoma. Hepatology 2013; 58: 205-217.
11) Casadei L, Calore F, Creighton CJ, Guescini M, Batte K, Iwenofu OH, Zewdu A, Braggio DA, Bill KL, Fadda P, Lovat F, Lopez G, Gasparini P, Chen JL, Kladney RD, Leone G, Lev D, Croce CM, Pollock RE. Exosome-Derived miR-25-3p and miR-92a-3p stimulate liposarcoma progression. Cancer Res 2017; 77: 3846-3856.
12) Ahmadi S, Sharifi M, Salehi R. Locked nucleic acid inhibits miR-92a-3p in human colorectal cancer, induces apoptosis and inhibits cell proliferation. Cancer Gene Ther 2016; 23: 199-205.
13) Liu Z, He F, OuYang S, Li Y, Ma F, Chang H, Cao D, Wu J. MiR-140-5p could suppress tumor proliferation and progression by targeting TGFBRI/SMAD2/3 and IGF-1R/AKT signaling pathways in Wilms' tumor. BMC Cancer 2019; 19: 405.
14) Wang H, Lou C, Ma N. MiR-140-5p alleviates the aggressive progression of Wilms' tumor through directly targeting gene. Cancer Manag Res 2019; 11: 1641-1651.
15) Zhu S, Zhang L, Zhao Z, Fu W, Fu K, Liu G, Jia W. MicroRNA-92a-3p inhibits the cell proliferation, migration and invasion of Wilms tumor by targeting NOTCH1. Oncol Rep 2018; 40: 571-578.
16) Wu S, Ou T, Xing N, Lu J, Wan S, Wang C, Zhang X, Yang F, Huang Y, Cai Z. Whole-genome sequencing identifies ADGRG6 enhancer mutations and FRS2 duplications as angiogenesis-related drivers in bladder cancer. Nat Commun 2019; 10: 720.

17) Luo LY, Kim E, Cheung HW, Weir BA, Dunn GP, Shen RR, Hahn WC. The tyrosine kinase adaptor protein FRS2 is oncogenic and amplified in high-grade serous ovarian cancer. Mol Cancer Res 2015; 13: 502-509.

18) Wang HF, Zhang YY, Zhuang HW, Xu M. MicroRNA-613 attenuates the proliferation, migration and invasion of Wilms' tumor via targeting FRS2. Eur Rev Med Pharmacol Sci 2017; 21: 3360-3369.

19) Li JH, Liu S, Zhou H, Qu LH, Yang JH. StarBase v2.0: decoding miRNA-ceRNA, miRNA-ncRNA and protein-RNA interaction networks from large-scale CLIP-Seq data. Nucleic Acids Res 2014; 42: D92-D97.

20) Dumba M, Jawad N, McHugh K. Neuroblastoma and nephroblastoma: an overview and comparison. Cancer Imaging 2014; 14 (Suppl 1): O15.

21) Cao XY, Sun ZY, Zhang LJ, Chen MK, Yuan B. MicroRNA-144-3p suppresses human neuroblastoma cell proliferation by targeting HOXA7. Eur Rev Med Pharmacol Sci 2019; 23: 716-723.

22) Liu T, Zhang X, Du L, Wang Y, Liu X, Tian H, Wang L, Li P, Zhao Y, Duan W, Xie Y, Sun Z, Wang C. Exosome-transmitted miR-128-3p increase chemosensitivity of oxaliplatin-resistant colorectal cancer. Mol Cancer 2019; 18: 43.

23) Wen Y, Han J, Chen J, Dong J, Xia Y, Liu J, Jiang Y, Dai J, Lu J, Jin G, Han J, Wei Q, Shen H, Sun B, Hu Z. Plasma miRNAs as early biomarkers for detecting hepatocellular carcinoma. Int J Cancer 2015; 137: 1679-1690.

24) Yingjie W, Zhengjun C, Axel U. EGFR and FGFR signaling through FRS2 is subject to negative feedback control by ERK1/2. Biol Chem 2003; 384: 1215-1226.

25) Zhang K, Chu K, Wu X, Gao H, Wang J, Yuan YC, Loera S, Ho K, Wang Y, Chow W, Un F, Chu P, Yen Y. Amplification of FRS2 and activation of FGFR/FRS2 signaling pathway in high-grade liposarcoma. Cancer Res 2013; 73: 1298-1307.